

http://periodicos.uem.br/ojs/acta ISSN on-line: 1807-863X

Doi: 10.4025/actascibiolsci.v41i1.43381



BOTANY

Anatomical and biochemical changes associated with the development and germination of *Araucaria angustifolia* seeds

Marília Shibata¹, Cileide Maria Medeiros Coelho^{2*}, Eder Carlos Schmidt³, Zenilda Laurita Bouzon³, José Marcello Salabert de Campos⁴ and Marcelo Maraschin⁵

¹Universidade Federal Rural da Amazônia, Capitão Poço, Pará, Brazil. ²Laboratório de Sementes, Universidade do Estado de Santa Catarina, Av. Luiz de Camões, 2090, 88520-000, Lages, Santa Catarina, Brazil. ³Laboratório de Biologia Celular Vegetal, Universidade Federal de Santa Catarina, Florianópolis, Santa Catarina, Brazil. ⁴Laboratório de Genética e Biotecnologia, Universidade Federal de Juiz de Fora, Juiz de Fora, Minas Gerais. Brazil. ⁵Laboratório de Morfogênese e Bioquímica Vegetal, Universidade Federal de Santa Catarina, Florianópolis, Santa Catarina, Brazil. *Author for correspondence. E-mail: cileide.souza@udesc.br

ABSTRACT. This study aimed at assessing the cell cycle, and anatomical and biochemical changes that the embryonic axis of *Araucaria angustifolia* undergoes during development, focusing on the maturation stage. During all development, cells exhibited intense metabolic activity with an abundance of mitochondria, lipid bodies, and vacuolated cells. The continued accumulation of starch and protein was observed by LM and TEM and indicated by spectra of FTIR. Cell differentiation of the procambium was observed with a thickening of the cell wall and the formation of resiniferous ducts. At Stage III and IV, cells exhibited structural changes such as altered or elongated mitochondria and presence of plastoglobules. These results suggest that there is a gradual transition from developmental metabolism to germination metabolism. Such changes can contribute to the rapid germination of seeds right after their dispersion, making it an ecological strategy to reduce post-dispersal exposure to predators and to avoid damage from reduced moisture.

Keywords: maturation; recalcitrant seed; light microscopy; transmission electron microscopy; flow cytometry.

Received on June 20, 2018. Accepted on March 29, 2019.

Introduction

Araucaria angustifolia (Bertol.) Kuntze is a native conifer with social, economic and ecological significance in southern Brazil (Wendling & Brondani, 2015). Clear-cutting and the spread of agriculture resulted in the inclusion of these species on the IUCN (International Union for Conservation of Nature) Red List of Threatened Species as critically endangered status (The International Union for Conservation of Nature [IUCN], 2018). However, their seeds are still an important source of income and food for many low-income families and small farmers (Zechini, Schussler, Silva, Mattos, Peroni, Mantovani, & Reis, 2012).

The maturation period of *A. angustifolia* seeds is between April and August (Mattos, 2011), which are classified as recalcitrant (Gasparin, Faria, José, & Hilhorst, 2017). In previous studies during the maturation period, morphological and physiological alterations in seeds were observed (Shibata, Coelho, & Steiner, 2013). However, the anatomical, biochemical and cell cycle changes that occur during the maturation of the seeds of these species are still unknown.

The maturation process in recalcitrant seeds might not be interrupted, even with the seeds still attached to the mother plant, due to the beginning of the germination process (Barbedo, Centeno, & Ribeiro, 2013). Species with recalcitrant seeds, such as *Inga vera* Willd. subsp. *affinis* (DC.) T. D. Penn. have been found to experience rapid temporary metabolic shifts during maturation with highly vacuolated cells, which suggest a continuum from maturation to germination prior to seed dispersion (Caccere, Teixeira, Centeno, Figueiredo-Ribeiro, & Braga, 2013). The embryonic axis of *Quercus ilex* L. has also shown the ability to accomplish signal transduction for seed germination during maturation, from the presence of the large number of biosynthesis and translation proteins (Sghaier-Hammami, Redondo-López, Valero-Galvàn, & Jorrín-Novo, 2016). Other species have accumulated starch or soluble carbohydrate during recalcitrant seed

Page 2 of 11 Shibata et al.

development to have the immediate energy for germination (Souza, Santos Dias, Pimenta, Almeida, Toledo Picoli, Pádua Alvarenga, & Silva, 2018; Mazlan, Aizat, Baharum, Azizan, & Noor, 2018). However, as for *A. angustifolia*, it is not known if the germination process may have started at the end of its development and have continued during storage (Araldi & Coelho, 2015).

Some changes are related to the germination process in recalcitrant seeds, such as formation of vacuoles, increases in the occurrence of mitochondria and in the extent endoplasmatic-reticulum development (Farrant, Pammenter, & Berjak, 1989; Obroucheva, Lityagina, Novikova, & Sin'kevich, 2012), differentiation of procambium in vascular tissues (Danial, Keng, Alwi, & Subramaniam, 2011), an increase in mitotic activity with changes in the 2C and 4C DNA content (Obroucheva, Sinkevich, & Lityagina, 2016), among others.

To provide more insights into maturation of *A. angustifolia* seeds during period of seeds collect from April, until the time they are dispersed, in the months of June/July, we conducted an investigation monitoring the seeds modifications of *A. angustifolia* to evaluate whether seeds exhibit a transition from developmental metabolism to germination metabolism although the seed is still connected to the mother plant. To answer this question we determined changes in anatomy, chemical composition and the cell cycle during the maturation period of seed development and we hypothesized that the germination process in the seeds of *A. angustifolia* begins when the seeds are still attached to the mother plant.

Material and methods

Cones (megastrobilus) of *A. angustifolia* var. indehicensis (Adan, Atchison, Reis, & Peroni, 2016) were collected from six mother-plants of natural population located in Santa Catarina, Brazil (27°55'30" S and 49°58'35" W at 1300 m in elevation) during March – June of 2014 and 2015. Cones were chosen based on the main color changes they experience during seed maturation: green (cones with predominantly green surface – Cotyledonary Stage), green-brownish (cones with green surface or with small brown spots for less than 50% of the total surface area – Stage II), brown-green (cones with green surface and large brown spots for more than 50% of the total surface area and exhibiting the start of dehiscence – Stage III) and brown (cones with a predominantly brown surface and undergoing dehiscence – Stage IV) (Figure 1).

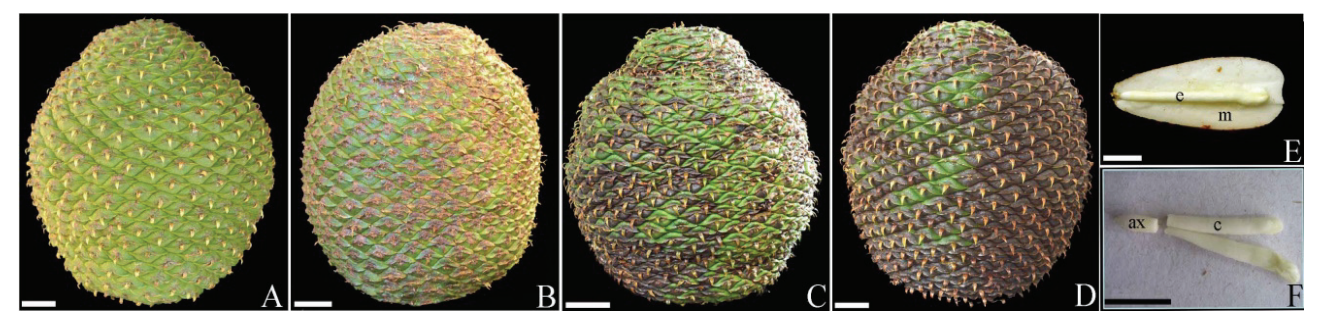


Figure 1. Alterations of cones of *Araucaria angustifolia*. Cotyledonary Stage: cones with green surface (A); Stage II: cones with green surface with brown small spots (B); Stage III: cones with green surface and brown large spots (C); Stage IV: cones with surface predominantly brown (D). Cross section of *A. angustifolia* seeds (E) showing the embryo (e) and megagametophyte (m). An embryo (F) showing the two cotyledons (c) and embryonic axis (ax). Bars: (A, B, C, D): 2 cm; (E, F): 1 cm.

After seeds were collected, their embryonic axis were extracted (Figure 1F) and submitted to light microscopy, transmission electron microscopy, DNA-content and infra red vibrational analyses.

Light microscopy

Transverse sections in the four development stages of *A. angustifolia* seeds collected in 2014 were used for the anatomical analyses. Embryonic axis were separated in plumule and hypocotyl-radicle axis fixed overnight in phosphate buffer 0.1 M (pH 7.2) containing 2.5 % formaldehyde at 4°C. Subsequently, the samples were dehydrated in an increasing series of aqueous ethanol solutions and then infiltrated with Historesin (Leica Historesin, Heidelberg, Germany). Semi-thin sections (4 µm thick) containing both plumule and hypocotyl-radicle axis were treated with different histochemical techniques. Periodic acid-

Schiff (PAS) was used to identify neutral polysaccharides (Gahan, 1984), 0.5% toluidine blue (TB-O) pH 3.0 (Merck Darmstadt, Germany) to identify acidic polysaccharides (Gordon & McCandless, 1973) and 0.4 % Coomassie Brilliant Blue (CBB) in Clarke's solution (Serva, Heidelberg, Germany) to identify proteins (Gahan, 1984). Sections were analyzed using an Olympus BX 41 light microscope equipped with Image Q Capture Pro 5.1 Software (QImaging Corporation, Austin, TX, USA).

Transmission electron microscopy

Semi-thin sections (2 µm) were made of samples collected in 2015 to compare with the sections from samples of 2014. Due to the similarity of the samples from the two years, those collected in 2015 were used for transmission electron microscopy (TEM). Samples of plumule and hypocotyl-radicle axis were fixed in 0.1 M sodium cacodylate buffer (pH 7.2) containing 4% formaldehyde and 2.5% glutaraldehyde for 12h (Schmidt, Scariot, Rover, & Bouzon, 2009). The material was post-fixed with 0.1 M sodium cacodylate buffer containing 1% osmium tetroxide for 4 hours, dehydrated in an increasing series of aqueous acetone solutions, and then embedded in Spurr's resin (Spurr, 1969). Ultra-thin sections (70 nm thick) were collected on grids and stained with aqueous uranyl acetate followed by lead citrate. Two grids were then examined using a JEM 1011 TEM (JEOL Ltd., Tokyo, Japan) at 80 kV.

DNA-content

To analyze the cell cycle, the apex of the embryonic axis was macerated on a Petri dish containing 1 mL of cold LB01 buffer using a scalpel blade to release the nuclei into suspension (Dolezel, Greilhuber, & Suda, 2007). The chopped tissue was aspirated through two layers of cheesecloth with a plastic pipette, filtered through a 50 mm nylon filter, and collected in a polystyrene tube. The nuclei were stained by adding 50 μ L of propidium iodide (1 mg mL⁻¹) and 5 μ L of RNase (100 μ g mL⁻¹) to each sample. The analysis was performed using a FACSCanto II (Becton, Dickinson and Company, USA) flow cytometer and histograms created with Cell Quest software.

Infrared vibrational analyses

Samples of *A. angustifolia* were submitted to Fourier transform infrared spectroscopy (FTIR) in a Bruker IFS 55 spectrophotometer with a glycerin-sulphate detector (DTGS) and attenuated total reflectance accessories (ATR, Golden Gate). One hundred and twenty-eight scans per sample were collected in spectral windows of 4000-500 waves cm⁻¹ at a resolution of 4 waves cm⁻¹. Three spectra were collected for each sample. Spectra were normalized, baseline corrected in the region of interest (3000 to 600 cm⁻¹) and processed with the aid of Essential Ftir software.

Statistical analysis

The FTIR dataset was subjected to principal components analysis (PCA) in R software (R Development Core Team, 2011).

The experimental design of the flow cytometry analysis was a completely randomized 2 x 4 factorial design (two years of harvest and four development stages) with three replicates of each treatment. The data were tested for normality and subjected to ANOVA. The means were compared by SNK's test at 5% significance.

Results

Anatomical changes to seeds

Plumule cells showed intense development when stained with TB-O due to cellular differentiation of the procambium and formation of resin ducts (Figure 2). A greenish-blue color shift was observed at Stage IV, indicating a thickening of the walls of tracheid cells containing phenolic and/or lignin compounds (Figure 2J). At Stage III, cells undergoing mitosis were recognized by the presence of two nuclei, thin cell walls between cells and separation of sister chromatids (Figure 2K).

PAS staining showed a positive reaction, indicating the presence of neutral polysaccharides. Such compounds were found primarily as starch grains and cell wall constituents. During development, starch

Page 4 of 11 Shibata et al.

grains and cytoplasm density increased from Stage II onward (Figure 2F). CBB staining revealed a large amount of protein throughout the cell cytoplasm and many white-appearing vacuoles, which increased both in number and size from Stage I onwards (Figure 2E). Hypocotyl-radicle axis cells showed few changes throughout seed development (data not shown).

TEM analysis of ultrastructure revealed a nucleus, secretory vesicles, abundant storage reserves, mitochondria and some Golgi bodies throughout development. The storage reserves of both hypocotyl-radicle axis and plumule cells included starch inside plastids and lipid bodies (Figure 3).

In Stages III and IV, the cells possessed relatively large vacuoles and a change in the appearance of mitochondria, with them being elongated and undergoing fission or fusion (Figure 3E and 3G). The mitochondrial matrices became increasingly devoid of internal detail with electron-transparent regions (Figure 3E). Plastoglobules were observed inside amyloplasts (Figure 3F).

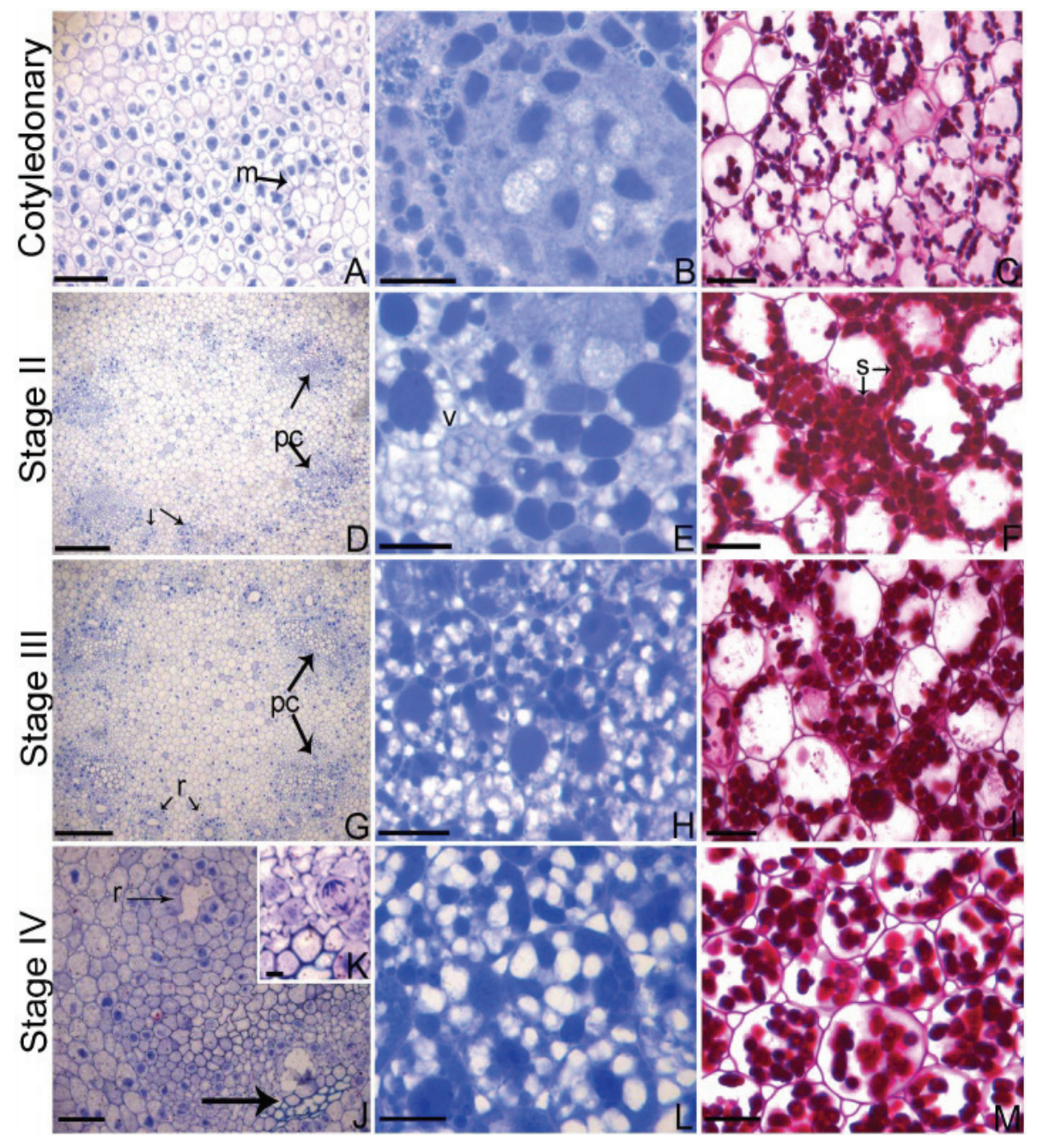


Figure 2. Light microscopy of *Araucaria angustifolia* plumule cells. Transversal sections stained with TB-O staining enhanced (pc) procambium, (r) resins ducts got bigger at Stages III and IV (G, J), a greenish-blue color shift at stage IV (J - arrow) and sister chromatids have separated and begin moving toward opposite poles of the cell (K). CBB staining showing vacuoles (v) and protein in blue (B, E, H, L). PAS staining, note the increased of starch grains (S) from Cotyledonary Stage to others stages. Bars: (A, J): 50 μm; (B, C, E, F, H, I, L, M): 20 μm; (D, G): 200 μm; (K): 0.3 μm.

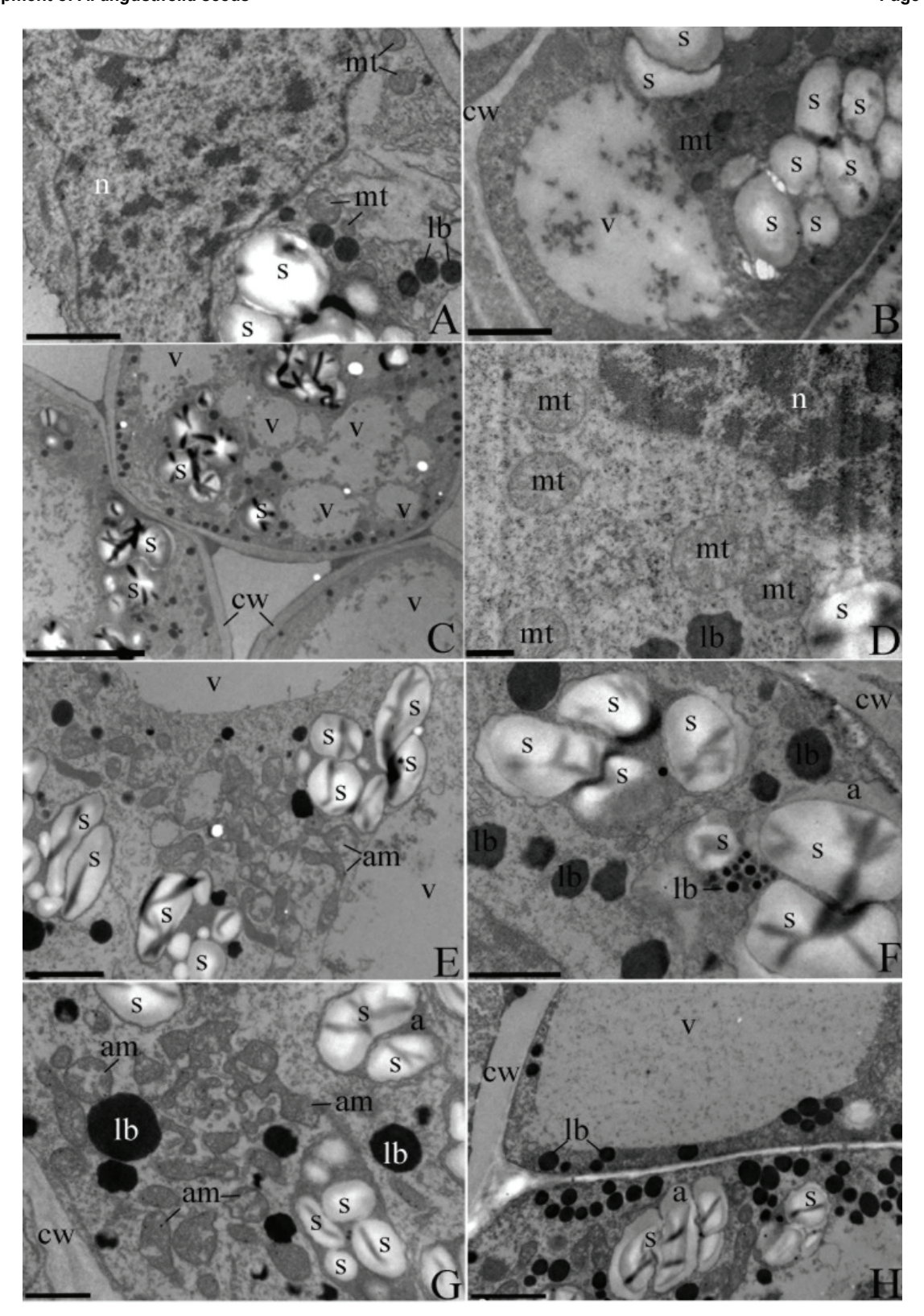


Figure 3. Transmission electron microscopy of *Araucaria angustifolia*. (A, C, E, G) Plumule and (B, D, F, H) hypocotyl-radicle axis cells at (A, B) Cotyledonary Stage, (C, D) Stage II, (E, F) Stage III and (G, H) Stage IV. Abbreviations: (a) amyloplast; (am) altered mitochondria; (cw) cell wall; (lb) lipid body; (mt) mitochondria; (n) nucleus; (s) starch granule; and (v) vacuole. Bars: (A, E, H): 2 μm; (B, F, G): 1 μm; (C): 5 μm; (D): 0.5 μm.

Flow cytometry analysis

Most of the nuclei of the embryonic axis of *A. angustifolia* contained 2C DNA, indicating that most of the cells were in the G1 phase of the cell cycle. Year of collection and stage of development did not exhibit interactions with 2 and 4C DNA values.

Page 6 of 11 Shibata et al.

A decrease in the content of 2C DNA from 82.58 to 77.35% was, however, observed from the Cotyledonary Stage to Stage IV. Nevertheless, the content of 4C DNA (G2 phase of the cell cycle) did not differ significantly between the Cotyledonary Stage and Stage IV, with it being 8.44 and 10.35%, respectively (Figure 4).

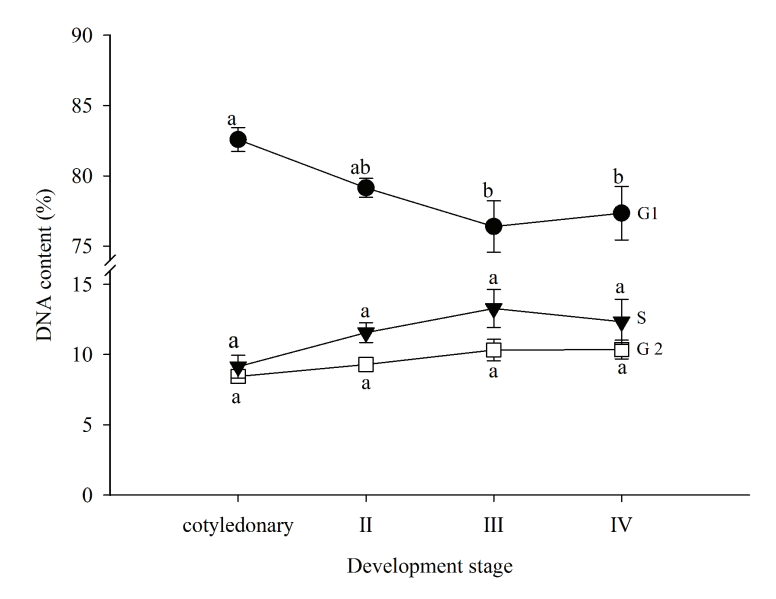


Figure 4. The cell cycle of *Araucaria angustifolia* embryonic axis. G1 phase (•): 2C DNA; S phase (▼): 2C/4C DNA and G2 phase (□): 4C DNA content at Cotyledonary Stage, II, III and IV. Bars represent standard error. The letters refer to the SNK's test (p < 0.05).

FTIR spectroscopy analyses

FTIR spectra of *A. angustifolia* showed vibrational band assignments for the major groups of biochemical components, with most of the absorption peaks being detected in the 3000-600 cm⁻¹ spectral window, indicating the presence of lipids (2924, 2854, and 1740 cm⁻¹), proteins (1650-1500 cm⁻¹), starch (1200-800 cm⁻¹) and phenolic compounds (900-690 cm⁻¹) at different developmental stages of seeds.

Three prominent areas in the lipid region were found at different development stages of *A. angustifolia* seeds: 2927, 2856, and 1745 cm⁻¹. Carbocyclic groups, associated with the axial deformation of functional group C=O, are typically found in fatty acids and can be detected in the regions of 3000-2800 cm⁻¹ (Lahlali et al., 2014) and 1740 cm⁻¹ (Kuhnen et al., 2010).

The two major vibrational bands of protein backbone are the Amide I and Amide II bands in the region 1500-1700 cm⁻¹ (Baker et al., 2014), which are mainly associated with the stretching vibration of C=O (Lahlali et al., 2014). At least one main absorption peak was observed at 1648 cm⁻¹ (Figure 5) in the Amide I region. The peaks observed in the 800-1200 cm⁻¹ spectral window indicated the presence of starch associated with the axial deformation of functional groups C-O, C-C and C-O-H and angular deformation of C-O-H (Warren, Gidley, & Flanagan, 2016).

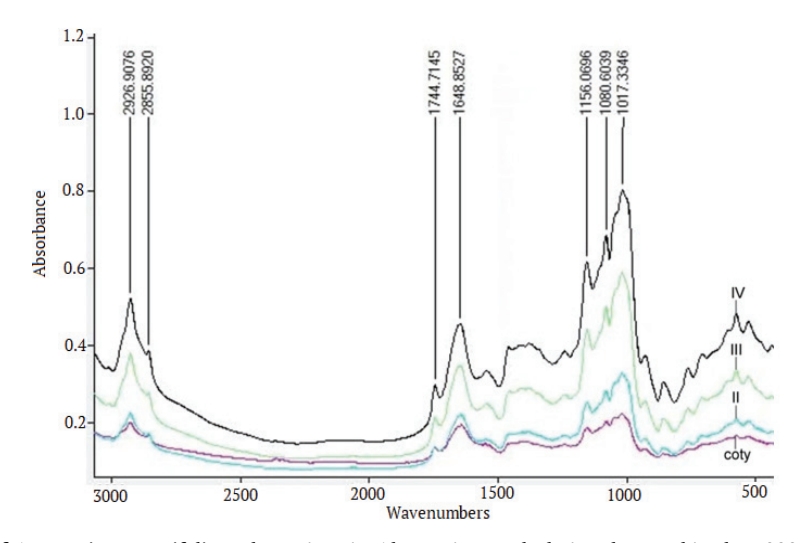


Figure 5. FTIR spectra of *Araucaria angustifolia* embryonic axis. Absorption peaks being detected in the 3000–600 cm⁻¹ spectral window at Cotyledonary Stage (coty), Stage II, III and IV.

The first two components of the principal components analysis (PCA) revealed clear discrimination of samples and explained 99.8% of the total variance of the FTIR dataset. The samples were dispersed along the first axis (PC1; 98% variance) and formed two groups with Cotyledonary Stage and Stage II in PC1-, and Stages III and IV in PC1+ (Figure 6).

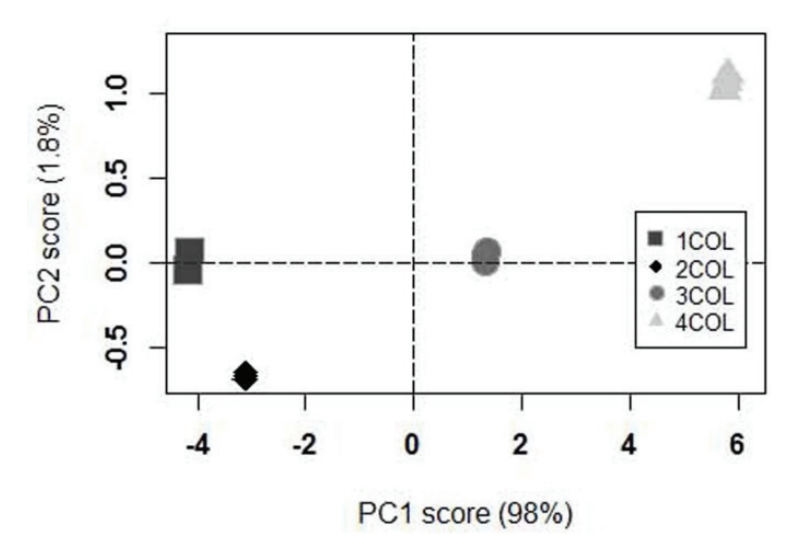


Figure 6. PCA of FTIR data set of *Araucaria angustifolia* embryonic axis at different development stages. 1COL: Cotyledonary Stage; 2COL: Stage II; 3COL: Stage III and 4COL: Stage IV.

Discussion

During the beginning of seed development there is intense cell-cycle activity in the cells. This cycle comprises the events necessary for cell division and is divided into two stages: interphase – subdivided into G1, S and G2 phases when there is intense metabolic activity due to DNA replication, growth and synthesis; and mitosis – the period wherein the genetic material is divided into two identical cells (Bewley, Bradford, Hilhorst, & Nonogaki, 2013). Recalcitrant seeds being dispersed with the majority of their cells in the G1 phase, such as what is seen in *Inga vera* (Faria, van Lammeren, & Hilhorst, 2004). The majority of the nuclei of the embryonic axis of *A. angustifolia* were in the G1 phase (DNA content 2C), as determined by flow cytometry analysis, while a decrease in the proportion of cells in the G1 phase was observed in Stages III and IV. Light microscopy found that in these stages some cells exhibited mitotic activity, as evidenced by the occurrence of nuclei being divided into two within the same cell (Figure 2K). These cells comprised part of the percentage of cells in the G2 phase as observed by flow cytometry (8 to 10%). There have been no previous reports regarding DNA content during *A. angustifolia* seed development; however, freshly harvested and germinated mature seeds have been found not to differ in 2C DNA content (Gasparin et al., 2017). These observations demonstrate that the seeds of *A. angustifolia*, even in the process of germination, seem to modify their DNA content late, probably after protrusion of the radicle.

The LM analysis observed cells stained with TB-O indicating the cellular differentiation of the procambium with a thickening of the cell wall and greater accumulation of lignin and/or phenolic compounds (Figure 2J). Such meristematic cells were observed in the early stages (Figure 2A and 2D), and the formation of resiniferous ducts in other stages (Figure 2G and 2J). The formation of resin is a defense strategy for plants (Mithöfer & Boland, 2012) and their initial formation can be considered preparation for the defense of the seed and its subsequent germination.

During all stages of development, plumule and hypocotyl-radicle axis cells of *A. angustifolia* seeds seemed to have intense metabolic activity, which could be deduced from the occurrence and frequency of mitochondria, Golgi bodies and lipid bodies. This elevated metabolism is frequently reported for recalcitrant seeds and is related to desiccation intolerance. Such seeds can be stored for a short period of time, making their conservation difficult, as with *A. angustifolia* (Silveira et al., 2008; Balbuena, Silveira, Junqueira, Dias, Santa-Catarina, Shevchenko, & Floh, 2009; Rogge-Renner, Steiner, Schmidt, Bouzon, Farias, & Guerra, 2013), *Inga vera* (Caccere et al., 2013), *Hevea brasiliensis* (Willd. ex A.Juss.) Müll.Arg. (Bonome, Moreira, de Oliveira, & Sotero, 2011) and *Aesculus chinensis* Bge. (Yu & Chen, 2011).

Page 8 of 11 Shibata et al.

The samples stained with CBB and PAS demonstrate the accumulation of proteins and starch during the stages analyzed (Figure 2L and 2M). These reserves were also observed using FTIR spectrophotometry (Figure 4), which has been previously used to analyze the composition of seeds (Kuhnen et al., 2010; Amir, Anjum, Khan, Pasha, & Nadeem, 2013; Barsberg, Rasmussen, & Kodahl, 2013; Araldi, Coelho, & Maraschin, 2016). Lipids, starch, proteins and phenolic compounds were present in all seed samples. These compounds can be easily converted into soluble substances and to contribute to the rapid transition from developmental metabolism to germination metabolism. Principal components analysis of FTIR demonstrated that the most important variables for PC1 were starch and proteins, which discriminated a group to the left formed by Cotyledonary Stage and Stage II, and a group to the right formed by Stage III and IV. These groups also showed similar features by LM and TEM analyses.

Furthermore, different mitochondrial morphologies seemed to occur more frequently in Stages III and IV (Figure 3C and 3D). In addition to the standard mitochondrial morphology with a typically cylindrical-shape, well-packed and organized cristae, elongated or altered mitochondria were observed often with matrices increasingly devoid of internal detail and with a modified electron-transparent region. These changes in mitochondria have been described for *A. angustifolia* in response to stress during in vitro culture conditions (Fraga, Vieira, Puttkammer, Oliveira, & Guerra, 2015). Thus, the presence of plastoglobules and altered mitochondria appears to be a response to the stress to which the seeds had been subjected. These events, along with the cellular differentiation and division observed by LM analysis, appear to be responses to the stress imposed on seeds by dispersion or in preparation to change metabolism.

Species with recalcitrant seeds, such as *Inga vera*, have exhibited rapid temporary metabolic shifts during maturation, moving directly from maturation to germination (Caccere et al., 2013). Early germination after being shed has been reported previously for *A. angustifolia* seeds, as well as its continuance during storage (Farrant et al., 1989; Garcia, Coelho, Maraschin, & Oliveira, 2014; Araldi & Coelho, 2015). This germination is rapid and non-homogeneous, furthermore, the seeds exhibit different post-harvest early-developmental categories after storage: seed with mature embryo; seeds with elongation along the embryonic axis; starting of root protrusion; advanced germination stage, with seedling shoots (Araldi & Coelho, 2015). Thus, these categories and our results support our hypothesis that there is a gradual transition from developmental metabolism to germination metabolism despite the fact that the seed is still connected to the mother plant and continue after storage. In addition, the seeds are able to germinate even under unfavorable conditions, once *A. angustifolia* seeds have a high moisture content and it's metabolism remains high after shedding.

The period of imbibition required by recalcitrant seeds at the onset of germination might be shorter than that of orthodox seeds, and they may germinate rapidly due to both having a high moisture content and an active metabolism, and so limited or no imbibition is required to initiate germination (Berjak & Pammenter, 1995), as it has been observed in *A. angustifolia* seeds (Balbuena et al., 2011). Thus, in latter development stages, *A. angustifolia* seeds could initiate germination without the requirement of additional water due to the fact that hypocotyl-radicle axis and plumule cells showed enhanced subcellular activity, including altered or elongated mitochondria, the presence of plastoglobules, vacuolation, cell division and differentiation.

Recalcitrant seeds transition quickly from development to germination, and they lack the ability to switch-off their metabolism after seed dispersal. However, some recalcitrant seeds modify their metabolism for germination even before dispersion, i.e., during seed development, which begins to mobilize both starch and proteins; highly vacuolated cells; biosynthesis and translation proteins (Caccere et al., 2013; Sghaier-Hammami et al., 2016). Such behavior facilitates the fast seedling establishment after their shedding. Therefore recalcitrant seeds do not constitute a persistent seed bank in the field, avoiding the risk of seed infection and predation.

Conclusion

Araucaria angustifolia seeds show a gradual transition from developmental metabolism to germination metabolism despite the fact that the seed is still connected to the mother plant. Such changes can be contributed to the rapid germination of seeds soon after their dispersion, making it an ecological strategy to reduce post-dispersal exposure to predators and to avoid damage from reduced moisture.

Acknowledgements

The authors would like to thank the LAMEB and LCME-UFSC for technical support during microscopy work. The first author thanks Marisa Santos *–Universidade Federal de Santa Catarina* for her helpful comments on the earlier version of the manuscript and *Programa de Bolsas Universitárias –* UNIEDU for providing a scholarship. The corresponding author thanks *Conselho Nacional de Desenvolvimento Científico e Tecnológico* (CNPq) for productivity scholarship. This article is part of Marilia Shibata's Doctoral Thesis.

Reference

- Adan, N., Atchison, J., Reis, M. S., & Peroni, N. (2016). Local Knowledge, Use and Management of Ethnovarieties of *Araucaria angustifolia* (Bert.) Ktze. in the Plateau of Santa Catarina, Brazil. *Economic Botany*, 70(4), 353-364. doi: 10.1007/s12231-016-9361-z
- Amir, R. M., Anjum, F. M., Khan, M. I., Khan, M. R., Pasha, I., & Nadeem, M. (2013). Application of fourier transform infrared (FTIR) spectroscopy for the identification of wheat varieties. *Journal of Food Science and Technology*, *50*(5), 1018-1023. doi: 10.1007/s13197-011-0424-y
- Araldi, C. G., & Coelho, C. M. M. (2015). Establishment of post-harvest early-developmental categories for viability maintenance of *Araucaria angustifolia* seeds. *Acta Botanica Brasilica*, *29*(4), 524-531. doi: 10.1590/0102-33062015abb0061
- Araldi, C. G., Coelho, C. M. M., & Maraschin, M. (2016). Metabolic profile of Brazilian pine embryos and megagametophyte of stored seeds. *African Journal of Agricultural Research*, *11*(9), 760-768. doi: 10.5897/AJAR2015.10054
- Baker, M. J., Trevisan, J., Bassan, P., Bhargava, R., Butler, H. J., Dorling, K. M., ... Martin, F. L. (2014). Using Fourier transform IR spectroscopy to analyze biological materials. *Nature Protocols*, *9*(8), 1771-1791. doi: 10.1038/nprot.2014.110
- Balbuena, T. S., Jo, L., Pieruzzi, F. P., Dias, L. L. C., Silveira, V., Santa-Catarina, C., ... Floh, E. I. S. (2011). Differential proteome analysis of mature and germinated embryos of *Araucaria angustifolia*. *Phytochemistry*, 72(4-5), 302-311. doi: 10.1016/j.phytochem.2010.12.007
- Balbuena, T. S., Silveira, V., Junqueira, M., Dias, L. L. C., Santa-Catarina, C., Shevchenko, A., & Floh, E. I. S. (2009). Changes in the 2-DE protein profile during zygotic embryogenesis in the Brazilian Pine (*Araucaria angustifolia*). *Journal of Proteomics*, 72(3), 337-352. doi: 10.1016/j.jprot. 2009.01.011
- Barbedo, C. J., Centeno, D. D. C., & Ribeiro, R. de C. L. F. (2013). Do recalcitrant seeds really exist? *Hoehnea*, 40(4), 583-595. doi: 10.1590/S2236-89062013000400001
- Barsberg, S., Rasmussen, H. N., & Kodahl, N. (2013). Composition of *Cypripedium calceolus* (Orchidaceae) seeds analyzed by attenuated total reflectance ir spectroscopy: in search of understanding longevity in the ground. *American Journal of Botany*, *100*(10), 2066-2073. doi: 10.3732/ajb.1200646
- Berjak, P., & Pammenter, N. W. (1995). Recalcitrant (desiccation-sensitive) seeds. In K. Olesen (Ed.), *Innovations in tropical tree seed technology* (p. 14-29). Arusha, TZ: Danilda Forest Seed centre.
- Bewley, J. D., Bradford, K., Hilhorst, H., & Nonogaki, H. (2013). *Seeds: physiology of development, germination and dormancy*. New York, NY: Springer.
- Bonome, L. T. S., Moreira, S. A. F., Oliveira, L. E. M. d., & Sotero, A. J. (2011). Metabolism of carbohydrates during the development of seeds of the brazilian rubber tree [*Hevea brasiliensis* (Willd. Ex Adr. de Juss) Muell.-Arg.]. *Acta Physiologiae Plantarum*, *33*(1), 211-219. doi: 10.1007/s11738-010-0540-8
- Caccere, R., Teixeira, S. P., Centeno, D. C., Figueiredo-Ribeiro, R. D. C. L., & Braga, M. R. (2013). Metabolic and structural changes during early maturation of *Inga vera* seeds are consistent with the lack of a desiccation phase. *Journal of Plant Physiology*, *170*(9), 791-800. doi: 10.1016/j.jplph.2013.01.002
- Danial, M., Keng, C. L., Alwi, S. S. R. S., & Subramaniam, S. (2011). Seed histology of recalcitrant *Eurycoma longifolia* plants during germination and its beneficial attribute for hairy roots production. *Journal of Medicinal Plants Research*, *5*(1), 93-98.
- Dolezel, J., Greilhuber, J., & Suda, J. (2007). Estimation of nuclear DNA content in plants using flow cytometry. *Nature Protocols*, *2*(9), 2233-44. doi: 10.1038/nprot.2007.310
- Faria, J. M. R., van Lammeren, A. M., & Hilhorst, H. W. M. (2004). Desiccation sensitivity and cell cycle aspects in seeds of *Inga vera* subsp. affinis. *Seed Science Research*, *14*(2), 165-178. doi: 10.1079/SSR2 004166

Page 10 of 11 Shibata et al.

Farrant, J. M., Pammenter, N. W., & Berjak, P. (1989). Germination-associated events and the desiccation sensitivity of recalcitrant seeds - a study on three unrelated species. *Planta*, *178*(2), 189-198. doi: 10.1007/BF00393194

- Fraga, H. P. F., Vieira, L. N., Puttkammer, C. C., Oliveira, E. M., & Guerra, M. P. (2015). Time-lapse cell tracking reveals morphohistological features in somatic embryogenesis of *Araucaria angustifolia* (Bert) O. Kuntze. *Trees*, *29*(5), 1613-1623. doi: 10.1007/s00468-015-1244-x
- Gahan, P. B. (1984). Plant histochemistry and cytochemistry: an introduction. London, UK: Academic.
- Garcia, C., Coelho, C. M. M., Maraschin, M., & Oliveira, L. M. (2014). Conservação da viabilidade e vigor de sementes de *Araucaria angustifolia* (Bert.) O. Kuntze durante o armazenamento. *Ciência Florestal*, *24*(4), 857-867. doi: 10.5902/1980509816586
- Gasparin, E., Faria, J. M. R., José, A. C., & Hilhorst, H. W. M. (2017). Physiological and ultrastructural responses during drying of recalcitrant seeds of Araucaria angustifolia. *Seed Science and Technology*, *45*(1), 112-129. doi: 10.15258/sst.2017.45.1.01
- Gordon, E. M., & McCandless, E. L. (1973). Ultrastructure and histochemistry of *Chondrus crispus* Stackhouse. *Proceedings of Nova Scotia Institute of Science*, *27*(1), 111-133.
- Kuhnen, S., Ogliari, J. B., Dias, P. F., Boffo, E. F., Correia, I., Ferreira, A. G., ... Maraschin, M. (2010). ATR-FTIR spectroscopy and chemometric analysis applied to discrimination of landrace maize flours produced in southern Brazil. *International Journal of Food Science and Technology*, *45*(8), 1673-1681. doi: 10.1111/j.1365-2621.2010.02313.x
- Lahlali, R., Jiang, Y., Kumar, S., Karunakaran, C., Liu, X., Borondics, F., ... Bueckert, R. (2014). ATR-FTIR spectroscopy reveals involvement of lipids and proteins of intact pea pollen grains to heat stress tolerance. *Frontiers in Plant Science*, *5*(1), 1-10. doi: 10.3389/fpls.2014.00747
- Mattos, J. R. d. (2011). O Pinheiro brasileiro. Florianópolis, SC: Ufsc.
- Mazlan, O., Aizat, W. M., Baharum, S. N., Azizan, K. A., & Noor, N. M. (2018). Metabolomics analysis of developing *Garcinia mangostana* seed reveals modulated levels of sugars, organic acids and phenylpropanoid compounds. *Scientia Horticulturae*, 233(1), 323-330. doi: 10.1016/j.scienta.2018.01.061
- Mithöfer, A., & Boland, W. (2012). Plant Defense Against Herbivores: Chemical Aspects. *Annual Review of Plant Biology*, 63(1), 431-450. DOI: 10.1146/annurev-arplant-042110-103854
- Obroucheva, N. V., Lityagina, S. V., Novikova, G. V., & Sin'kevich, I. A. (2012). Vacuolar status and water relations in embryonic axes of recalcitrant *Aesculus hippocastanum* seeds during stratification and early germination. *AoB PLANTS*, *12*(1), 1-14. DOI: 10.1093/aobpla/pls008
- Obroucheva, N., Sinkevich, I., & Lityagina, S. (2016). Physiological aspects of seed recalcitrance: a case study on the tree *Aesculus hippocastanum*. *Tree Physiology*, *36*(9), 1127-1150. doi: 10.1093/treephys/tpw037
- R Development Core Team. (2011). *R: A language and environment for statistical computing*. Vienna, AT: R Foundation for Statistical Computing.
- Rogge-Renner, G. D., Steiner, N., Schmidt, É. C., Bouzon, Z. L., Farias, F. L., & Guerra, M. P. (2013). Structural and component characterization of meristem cells in *Araucaria angustifolia* (Bert.) O. Kuntze zygotic embryo. *Protoplasma*, *250*(3), 731-739. doi: 10.1007/s00709-012-0457-8
- Schmidt, É. C., Scariot, L. A., Rover, T., & Bouzon, Z. L. (2009). Changes in ultrastructure and histochemistry of two red macroalgae strains of *Kappaphycus alvarezii* (Rhodophyta, Gigartinales), as a consequence of ultraviolet B radiation exposure. *Micron*, *40*(8), 860-869. doi: 10.1016/j.micron.2009. 06.003
- Sghaier-Hammami, B., Redondo-López, I., Valero-Galvàn, J., & Jorrín-Novo, J. V. (2016). Protein profile of cotyledon, tegument, and embryonic axis of mature acorns from a non-orthodox plant species: *Quercus ilex. Planta*, 243(2), 369-396. doi: 10.1007/s00425-015-2404-3
- Shibata, M., Coelho, C. M. M., & Steiner, N. (2013). Physiological quality of *Araucaria angustifolia* seeds at different stages of development. *Seed Science and Technology*, *41*(11), 214-224. doi: 10.15258/sst.2013.41. 2.04
- Silveira, V., Santa-Catarina, C., Balbuena, T. S., Moraes, F. M. S., Ricart, C. A. O., Sousa, M. V., ... Floh, E. I. S. (2008). Endogenous abscisic acid and protein contents during seed development of *Araucaria angustifolia*. *Biologia Plantarum*, *52*(1), 101-104. doi: 10.1007/s10535-008-0018-3

- Souza, G. A. d., Santos Dias, D. C. F. d., Pimenta, T. M., Almeida, A. L., Toledo Picoli, E. A. d., Pádua Alvarenga, A. d., & Silva, J. C. F. d. (2018). Sugar metabolism and developmental stages of rubber tree (*Hevea brasiliensis* L.) seeds. *Physiologia Plantarum*, *162*(4), 495-505. doi: 10.1111/ppl.12650
- Spurr, A. R. (1969). A low-viscosity epoxy resin embedding medium for electron microscopy. *Journal of Ultrastructure Research*, *26*(1-2), 31-43. doi: 10.1016/S0022-5320(69)90033-1
- The International Union for Conservation of Nature [IUCN]. (2018). *The IUCN red list of threatened species*. Retrieved from May 25, 2018 on www.iucnredlist.org
- Warren, F. J., Gidley, M. J., & Flanagan, B. M. (2016). Infrared spectroscopy as a tool to characterise starch ordered structure A joint FTIR-ATR, NMR, XRD and DSC study. *Carbohydrate Polymers*, *139*(1), 35-42. doi: 10.1016/j.carbpol.2015.11.066
- Wendling, I., & Brondani, G. E. (2015). Vegetative rescue and cuttings propagation of *Araucaria angustifolia* (Bertol.) Kuntze. *Revista Árvore*, *39*(1), 93-104. doi: 10.1590/0100-67622015000100009
- Yu, F., & Chen, S. (2011). Morphological and biochemical changes of *Aesculus chinensis* seeds in the process of maturation. *New Forests*, *43*(4), 429-440. doi: 10.1007/s11056-011-9289-1
- Zechini, A. A., Schussler, G., Silva, J. Z., Mattos, A. G., Peroni, N., Mantovani, A., & Reis, M. S. dos. (2012). Produção, comercialização e identificação de variedades de pinhão no entorno da Floresta Nacional de Três Barras–SC. *Revista Biodiversidade Brasileira*, *2*(2), 74-82.